On the uncertainty of initial condition and initialization approaches in variably saturated flow modeling

Danyang Yu[1], Jinzhong Yang[1], Liangsheng Shi[1], Qiuru Zhang[1], Kai Huang[2], Yuanhao Fang[3], Yuanyuan Zha[1*]

[1]State Key Laboratory of Water Resources and Hydropower Engineering Sciences, Wuhan University, Wuhan, Hubei 430072, China

[2] Guangxi Hydraulic Research Institute, Nanning, Guangxi 530023, China

[3] School of Earth Sciences and Engineering, Hohai University, Nanjing 210098, China

* *Corresponding author*: Yuanyuan Zha (zhayuan87@whu.edu.cn)

Abstract:

Soil water movement has direct effects on environment, agriculture and hydrology. Simulation of soil water movement requires accurate determination of model parameters as well as initial and boundary conditions. However, it is difficult to obtain the accurate initial soil moisture/matric potential profile at the beginning of simulation time, making it necessary to run the simulation model from arbitrary initial condition until the uncertainty of initial condition (UIC) diminishes, which is often known as "warming up". In this paper, we compare two commonly used methods for quantifying the UIC (one is based on running a single simulation recursively across multiple hydrological years, and the other is based on Monte-Carlo simulations with realization of various initial conditions) and identify the "warm-up" time t_{wu} (minimum time required to eliminate the UIC by warming up the model) required with different soil textures, meteorological conditions, and soil profile lengths. Then we analyze the effects of different initial conditions on parameter estimation within two data assimilation frameworks (i.e, ensemble Kalman filter and iterative ensemble smoother) and assess several existing model initializing methods that uses available data to retrieve initial soil moisture profile. Our results reveal that Monte-Carlo simulations and the recursive simulation over many years can both demonstrate the temporal behavior of UIC and a common threshold is recommended to determine t_{wu}. Moreover, the relationship between t_{wu} for variably saturated flow modeling and the model settings (soil textures, meteorological conditions and soil profile length) are quantitatively identified. In addition, we propose a "warm-up" period before assimilating data in order to obtain a better performance for parameter and state estimation.

Key words: Variably saturated flow; Initialization method; Initial condition uncertainty; Data assimilation; Soil moisture

1. Introduction

Understanding the movement of soil water is of great importance due to its direct effects across different disciplines, such as environment, agriculture and hydrology (Doussan et al., 2002). However, modeling of flow in variably saturated soil is complicated by many difficulties, including highly variable and nonlinear physical processes, as well as limited information about the soil hydraulic properties, initial conditions, and boundary conditions (DeChant, 2014; Rodell et al., 2005; Seck et al., 2014; Bauser et al., 2016; Li et al., 2012). The soil hydraulic parameter uncertainty is identified as a major uncertainty source in vadose zone hydrology and many studies have been focused on this topic. A highly relevant research area, inverse modeling, has been developed to reduce the uncertainty of parameter by incorporating observational data (Erdal et al., 2014; Montzka et al., 2011; Wu and Margulis, 2013; Wu and Margulis, 2011). Boundary conditions also introduce uncertainty during the simulation of soil water flow (Ataie-Ashtiani et al., 1999; Forsyth et al., 1995; Szomolay, 2008). For instance, the uncertainty introduced by flawed/noise-contaminated meteorological data or fluctuating groundwater table, has been investigated in the past (Freeze, 1969; French et al., 1999; van Genuchten and Parker, 1984; Ji and Unger, 2001; Xie et al., 2011).

Many publications have addressed the issue of the uncertainty of initial condition (UIC) in modeling soil water movement. For example, Walker and Houser (2001) compared the simulation with degraded soil moisture initial condition to that with true initial condition and found the discrepancy did not fade away even after one month. Then, Mumen (2006) concluded that the initial soil water state was one of the most important factors for estimating soil moisture in the case of bare soil. Chanzy et al. (2008) tested three initial water potential profiles and found that initialization had a strong impact on the soil moisture prediction. These studies showed that the incorrect initial condition may lead to false results. Based on the availability of information, different initialization approaches can be used for constructing initial conditions, e.g., an arbitrary uniform profile (Chanzy et al., 2008; Das and Mohanty, 2006; Varado et al, 2006), a linear interpolation with in situ observation (Bauser et al., 2016), a steady-state soil moisture profile induced with a constant infiltration flux (Freeze, 1969). All of the approaches involve great uncertainties due to nonlinearity of soil moisture profile, observation error, or inaccurate boundary condition. As a result, it is crucial to explore the effects of UIC on model outputs and compare the uncertainties inherited from various initialization approaches.

Besides the simple initialization methods referred above, another common approach is to obtain initial condition inherited from the warm-up model with preceding meteorological data. Starting from an arbitrary initial condition, this approach runs the model using a certain period (i.e., warm-up time t_{wu}) of meteorological data until the model state (e.g., soil moisture) reaches an equilibrium state, which is defined as the state when the uncertainty of state originated from UIC is negligible during simulation. The equilibrium state can be obtained by either running Monte-Carlo simulations until the states from different initial conditions converge to the same value (hereafter referred to as Monte-Carlo method) (Chanzy et al., 2008), or running a single simulation for several years by repeating one-year or multiple-year meteorological condition until the state at an arbitrary date ceases to vary from year to year (Spin-up method) (Dechant and Moradkhani, 2011; Seck et al., 2014). Spin-up method is widely used in large-scale hydrological model due to its smaller computational cost, while the less-common Monte-Carlo method has the merit of quantifying UIC explicitly at arbitrary time, which can be potentially used to construct state covariance matrix for data assimilation. To the best of our knowledge, there is no comparison made between these two methods to date. Finding an equivalency between these two methods is beneficial for linking initialization methods and data assimilation techniques. Moreover, the determination of warm-up time t_{wu} is crucial to the success of this approach (Ajami et al., 2014; Rahman and Lu, 2015). An underestimation of t_{wu} may bring uncertainty from arbitrarily-specified initial condition prior to initialization, while a large t_{wu} leads to higher computational demands (Rodell et al., 2005). A variety of modeling settings, such as soil hydraulic properties, meteorological conditions, and soil profile lengths, have strong influences on t_{wu} (Ajami et al., 2014; Cosgrove et al., 2003; Lim et al., 2012a; Walker and Houser, 2001). Thus, the determination of t_{wu} should be investigated thoroughly with different settings.

As well as model predictions, UIC also has considerable effects on parameter estimation. One of the commonly-used inverse methods in the field of vadose zone hydrology is data assimilation approach (Vereecken et al., 2010; Chirico et al., 2014; Medina et al., 2014a, 2014b). Previous studies showed that a poor initial soil moisture profile can be corrected by assimilating near-surface measurements (Galantowicz et al., 1999; Walker and Houser, 2001; Das and Mohanty, 2006). Oliver and Chen (2009) discussed several possible approaches to improve the performance of data assimilation through improved sampling of the initial ensemble, and suggested the use of the pseudo-data. Recently, Tran et al. (2013) found that decreasing assimilation interval could improve the soil moisture profile results induced by wrong initial condition and Bauser et al. (2016) has addressed the importance of UIC in data assimilation framework. However, these preliminary investigations of the influence of UIC on data assimilation results are degraded by the narrow choice of initialization and data assimilation methods, and the lack of comprehensive assessment of the temporal evolution of state/parameter uncertainty when UIC and the parameter uncertainty coexist. For instance, during data assimilation, the initial ensemble is often assumed to be known without uncertainty (Shi et al., 2015) or created by adding Gaussian noise to the initial estimate (Huang et al., 2008), both of which may result in false outputs. The researches mentioned above are all based on a sequential data assimilation approach (i.e., ensemble Kalman filter, or EnKF (Walker and Houser, 2001; Oliver and Chen, 2009)), which incorporates observation in a sequential fashion, so the effect of UIC can be eliminated quickly. Compared to EnKF, an iterative ensemble smoother (IES), which assimilates all data available simultaneously, can obtain reasonably good history-matching results and performs better in strongly nonlinear problems (Chen and Oliver, 2013). However, IES utilize all the observation simultaneously at every iteration and UIC may have a more persistent effect on IES. Thus, a systematical analysis for the effects of UIC and initialization methods within various data assimilation frameworks is necessary and obliged.

The objectives of this paper, therefore, are to: a) compare the temporal evolution of UIC with two common methods (Spin-up method and Monte-Carlo method) and identify the warm-up time t_{wu} under different soil hydraulic parameters, meteorological conditions and soil profile lengths; b) analyze the effects of different initial conditions on parameter estimation during data assimilation with EnKF or IES, and c) propose a selection scheme for choosing a suitable approach of initializing variably saturated flow models within different data assimilation frameworks to minimize the influence of UIC. We first summarize the governing equations of variably saturated flow and method of UIC quantification in Section 2. Then we present results of synthetic simulations designed to investigate the propagation of UIC under different scenarios in Section 3, which is complemented by the results for field data in Section 4. Finally, we present our conclusions in Section 5.

2. Method

2.1 One-dimensional soil water movement

Richards' equation can be used to describe the one-dimensional, vertical soil water movement, which is given as:

$$\frac{\partial \theta}{\partial t} = \frac{\partial}{\partial z}\left[K\left(\frac{\partial h}{\partial t}+1\right)\right] \tag{1}$$

where h [L] represents the pressure head; θ [-] denotes volumetric soil moisture; t [T] indicates the time; z [L] is the spatial coordinate taken positive upward; K [LT^{-1}] denotes the unsaturated hydraulic conductivity. The solution of one-dimensional Richards' equation is numerically solved by a noniterative numerical scheme, which was originally proposed in Ross (2003) and Ross (2006). By using the primary variable switching scheme, this scheme uses the soil moisture as the unknown variable for unsaturated nodes and pressure head for saturated nodes (Zha et al., 2013). It can greatly reduce the computational cost of variably saturated flow modeling in soils under atmospheric boundary condition, where alternative drying-wetting conditions are often encountered.

To obtain the solution of Eq. (1), the knowledge of functions K and θ versus h must be required. In this study, we use the van Genuchten-Mualem model (van Genuchten, 1980; Mualem, 1976) to describe these relationships,

$$\theta(h) = \theta_r + \frac{\theta_s - \theta_r}{\left[1+|\alpha h|^n\right]^m} \tag{2}$$

$$K(\theta) = K_s S_e^{0.5}[1-(1-S_e^{1/m})^m]^2 \tag{3}$$

where K_s [LT^{-1}] denotes the saturated hydraulic conductivity; θ_s and θ_r represent the saturated and residual soil moistures, respectively; parameters α [L^{-1}] and n are related to the measure of the pore-size density functions and m=1-1/n (n>1); the effective saturation degree S_e is defined as $S_e=(\theta-\theta_r)/(\theta_s-\theta_r)$.

Initial and boundary conditions are needed to solve the one-dimensional Richards' equation. The initial condition could be the states of soil moisture

$$\theta(z,t)\big|_{t=0} = \theta_0(z) \tag{4}$$

where $\theta_0(z)$ is the initial soil moisture profile.

State-dependent, atmospheric boundary condition can be described as (Šimůnek et al., 2013):

$$|q| = \left| -K\frac{\partial h}{\partial z} - K \right| \le \left| E_p - P_p \right| \tag{5}$$

$$h_m > h > h_c \tag{6}$$

where q [LT^{-1}] is the Darcian flux at the soil surface; E_p [LT^{-1}] denotes the potential evaporation; P_p [LT^{-1}] represents the precipitation intensity; h_m [L] and h_c [L] are maximum and minimum pressure heads allowed at the soil surface, respectively. The value of h_m is set to 0, whereas h_c is determined as -100 m.

The bottom boundary condition is the free drainage boundary:

$$\left.\frac{\partial h}{\partial z}\right|_{z=z_N} = 0 \tag{7}$$

where z_N is the depth of bottom boundary.

2.2 UIC quantification

The investigation of uncertainty in this study includes model states (e.g., soil moisture) and model parameters, where UIC is a special case of state uncertainty at t=0. The analysis is twofold. First, we consider a particular situation when UIC is the only uncertain source and all the model parameters are known. Thus, the choice of initial conditions is solely responsible for the accuracy of the model outputs. In this case, the temporal decay of UIC can be clearly demonstrated by utilizing Spin-up or Monte-Carlo methods. Second, a more complex and realistic situation, including both uncertain initial condition and model parameters, is considered during the data assimilation of soil moisture observation. UIC and data assimilation are smoothly combined in our approach since we choose Monte-Carlo-based methods (EnKF and IES). At t=0, we generate an ensemble of soil moisture profiles based on one initialization method (which introduces UIC), and use this ensemble to initiate the data assimilation (assimilate observations and estimate parameter). Finally, we can evaluate our data assimilation performance based on different initializing methods.

2.2.1 The indexes of Spin-up and Monte-Carlo methods

The uncertainty of initial condition can be measured by the percent change PC for Spin-up method (Ajami et al., 2014; Seck et al., 2014) or the ensemble spread S_p for Monte-Carlo method (Reichle and Koster, 2003). Percent change is an index that reflects the deviation of soil moisture between two adjacent years in a recursive run after a period of warm-up time t_{wu}, which could be calculated as:

$$PC(t) = 100\left|\frac{M(t) - M(t+12)}{M(t+12)}\right| \tag{8}$$

where $M(t)$ and $M(t+12)$ are the monthly averaged soil moistures after model spin-up for t months and t+12 months (de Goncalves et al., 2006).

The ensemble spread (S_p), calculated as a square root of averaged variance over all interested nodes, is an index to quantify the difference among various realizations in Monte Carlo simulation, and it is given as:

$$S_p(k) = \sqrt{\frac{1}{N(N_e - 1)}\sum_{i=1}^{N}\sum_{j=1}^{N_e}(y_{i,j,k}^a - \langle y_{i,k}^a \rangle)^2} \tag{9}$$

where $y_{i,j,k}^a$ is nodal soil moisture value; $\langle y_{i,k}^a \rangle$ is the ensemble mean of $y_{i,j,k}^a$; i = 1, 2, …, N are the nodes of interest (can be part of the profile); j=1, 2, …, N_e is the ensemble number index; N_e is the ensemble size, which is taken as 300 in this study based on sensitivity analysis of the ensemble size on the calculated results. When N = 1, the concept of $S_p(k)$ is equivalent to the standard deviation of y_k^a at one location and time t_k.

2.2.2 Data assimilation approaches

We employ EnKF and IES for data assimilation in this study. Fig. 1 illustrates the basic ideas and differences of the two methods.

EnKF approach was first proposed by Evensen (1994) and has been widely used in variably saturated flow problems (Huang et al., 2008; De Lannoy et al., 2007). This approach is a sequential data assimilation method (as shown in Fig. 1(a)) which incorporates observations into the model in order.

In this part, we assume that hydraulic parameters K_s, α, and n are unknown, while the other parameters θ_r and θ_s are deterministic. The vector of parameter and state is described as,

$$\mathbf{y}_k = [\mathbf{m}_k, \mathbf{u}_k]^T \tag{10}$$

where $\mathbf{m}_k$ is the parameter vector (i.e., K_s, α, and n), $\mathbf{u}_k$ are state variables (i.e., soil moisture) at time t_k, the dimension of y_k is N_y: N_y= N_m+ N_d, where N_m indicates the amount of the parameters to be estimated;

N_d are the number of nodes of the numerical model. The updated soil moisture ensemble can be converted to pressure head to drive the model. The observation vector can be defined as,

$$\mathbf{d}_{j,k} = \mathbf{d}_k + \boldsymbol{\varepsilon}_{j,k} \tag{11}$$

where $\mathbf{d}_k$ denotes the observation at time t_k; $\boldsymbol{\varepsilon}_{j,k}$ (j=1, 2, …, N_e) are independent Gaussian noises added to the observations; $\mathbf{d}_{j,k}$ is the observation vector for ensemble index j at time t_k. Based on the differences of model forecast and observations, the state-parameter vector can be updated as:

$$\mathbf{y}^a_{j,k} = \mathbf{y}^f_{j,k} + \mathbf{K}_k(\mathbf{d}_{j,k} - \mathbf{H}\mathbf{y}^f_{j,k}) \tag{12}$$

where $\mathbf{y}^f_{j,k}$ denotes the estimated or initially guessed values of parameter and state, while $\mathbf{y}^a_{j,k}$ is the updated estimates; $\mathbf{H}$ is an observation operator, linking the relationship between the state-parameter vector and the observation vector. $\mathbf{K}$ represents the Kalman gain matrix, which can be calculated as,

$$\mathbf{K}_K = \mathbf{C}^f_k\mathbf{H}^T[\mathbf{H}\mathbf{C}^f_k\mathbf{H}^T + \mathbf{C}_{D_K}]^{-1} \tag{13}$$

where $\mathbf{C}_{D_k}$ indicates the covariance matrix of observed data errors, while $\mathbf{C}^f_k$ is the error covariance matrix of forecast ensemble, given by

$$\mathbf{C}^f_k \approx \frac{1}{N_e - 1}\sum_{j=1}^{N_e}\left\{\left[\mathbf{y}^f_{j,k} - \left\langle \mathbf{y}^f_k \right\rangle\right]\left[\mathbf{y}^f_{j,k} - \left\langle \mathbf{y}^f_k \right\rangle\right]^T\right\} \tag{14}$$

where $\left\langle \mathbf{y}^f_k \right\rangle$ is the ensemble mean of $\mathbf{y}^f_k$.

Compared to EnKF, IES gives a better estimate by taking all the available observation into consideration (van Leeuwen and Evensen, 1996), as presented in Fig. 1(b). Thus, it can keep the overall consistency of parameters and state variables over time effectively and has been increasingly used to solve the parameter estimation problem in hydrology (Crestani et al., 2013; Emerick and Reynolds, 2013). By calculating iteratively, the nonlinear relationship between observation and parameter is linearized and the information content of the observations can be fully utilized (Chen and Oliver, 2013). In this case, we write the analyzed vector of model parameters $\mathbf{m}^r_j$, as

$$\mathbf{m}^{r+1}_j = \mathbf{m}^r_j + \mathbf{K}^r(\mathbf{d}^r_j - \mathbf{H}\mathbf{m}^r_j) \tag{15}$$

The notation is similar to the one presented for EnKF, where r is the iteration index; $\mathbf{m}^r_j$ is the initially guessed or estimated parameters for realization j at iteration r; $\mathbf{m}_j^{r+1}$ is the updated estimates for realization j by conditioning on the observed information at iteration r. It should be noted that the $\mathbf{d}_j^r$ and $\mathbf{Hm}_j^r$ denotes the total number of observations and predicted data at iteration r, which is different from EnKF. The Kalman gain $\mathbf{K}$ is defined as,

$$\mathbf{K}^r = \mathbf{C}_r^f\mathbf{H}^T[\mathbf{H}\mathbf{C}_r^f\mathbf{H}^T + \mathbf{C}_D + \lambda\mathrm{diag}(\mathbf{H}\mathbf{C}_r^f\mathbf{H}^T)]^{-1} \tag{16}$$

where $\mathbf{C}_r^f\mathbf{H}^T$ is the cross-covariance matrix between the prior vector of model and the vector of predicted data at iteration r; $\mathbf{H}\mathbf{C}_r^f\mathbf{H}^T$ is the auto-covariance matrix of predicted data at iteration r and $\mathbf{C}_D$ is the covariance matrix of observed data errors. λ donates a dynamic stability multiplier, which is set as 10 initially, and can be adjusted adaptively according to the data misfit at every iteration. diag ($\mathbf{H}\mathbf{C}_r^f\mathbf{H}^T$) is a diagonal matrix with the same diagonal elements as $\mathbf{H}\mathbf{C}_r^f\mathbf{H}^T$. Mathematically, the dynamic stabilizer term facilitates the solution switching between the Gauss-Newton solution and the steepest-descent method, which is known as the Levenberg-Marquardt approach (Pujol, 2007).

2.3.3 Quantitative index for data assimilation

To assess model parameter and state estimations, root mean square of estimated parameters ($RMSE_m$) and soil moisture ($RMSE_{obs}$), and the relative error index (RE) are computed as follows:

$$RMSE_m = \sqrt{\frac{1}{N_e}\sum_{j=1}^{N_e}(m_j^E - m^T)^2} \tag{17}$$

$$RMSE_{obs} = \sqrt{\frac{1}{N_{obs}}\sum_{n=1}^{N_{obs}}(d_n^e - d_n^{obs})^2} \tag{18}$$

$$RE = \frac{RMSE_m^e}{RMSE_m^p} \tag{19}$$

where m_j^E represents the estimated parameter of realization j at the last simulation day (EnKF) or the last iteration (IES); m^T represents the true parameter listed in Table 1. d_n^e and d_n^{obs} indicate the predicted and measured soil moistures, respectively. N_{obs} is the amount of observations. $RMSE_m^e$ and

$RMSE_m^p$ represent the *RMSE* of the estimated and prior parameters. *RE* varies from 0 to positive infinity. As *RE* approaches to 0, the analysis result is close to the truth, but a large value of *RE* (more than 1) indicates a bad parameter estimation. Compared with the $RMSE_m$, this index can better present the improvement of parameter estimation during data assimilation.

3. Numerical examples

A series of synthetic numerical experiments are performed in this section. In Section 3.1, we give a general description of the numerical experiments. In order to gain a better understanding of the propagation of the UIC, all the hydraulic parameters (i.e., K_s, α and n) are deterministic and the UIC is the only uncertainty source in Section 3.2. Finally, the numerical cases are designed to evaluate performances of data assimilation algorithms combined with various initialization methods in Section 3.3, in which the parameter uncertainty is taken into consideration in conjunction with UIC.

3.1 General description of model inputs

As shown in Table 1, four soils (Sand, Loam, Silt and Clay loam) are chosen in this study to explore the impacts of soil hydraulic property on UIC. The values of hydraulic parameters are determined according to Carsel and Parrish (1988). Besides, the effects of meteorological condition are also considered: M-AC, M-SC and M-HC in Fig. 2 represent three sets of precipitation and potential evaporation data from three different regions (arid region, semi-arid region and humid region) in China.

Unless otherwise specified, a uniform soil profile with the 50% relative saturation (a value of 0.254 for Loam) is chosen as the initial condition (IC-HfSatu). The soil profile is set to be 300-cm thick and is filled with Loam. The flow domain is discretized into 60 grids with a grid size of 5 cm which has been proved to be sufficient for evaluating UIC in our study (results not shown). Besides, the total simulation time during the synthetic simulation is one year (365 days). In addition, the default upper and bottom boundaries are set to be M-SC and free drainage boundary, respectively. Other specifications and assumptions for our model simulation runs are given in Table 2.

3.2 The temporal evolution of UIC

3.2.1 Comparison of UIC quantification methods

A synthetic experiment is conducted to compare two methods (i.e., Spin-up method and Monte-Carlo method) in quantifying UIC. Using the Spin-up method, the first case runs a single simulation for 10 years by repeating the preceding meteorological condition starting with IC-HfSatu (Fig. 3(a)), and the percentage cutoff *PC* is calculated. In the second case, the Gaussian noise with a standard deviation of 3% (determined according to the observation error of soil moisture) is added to the IC-HfSatu to generate an ensemble with different initial soil moisture profiles. Then we run different model realizations (Fig. 3(b)). Finally, the *PC* and S_p values of the two cases versus time are compared in Fig. 3(c).

As shown in Fig. 3(a), there is a visible difference between the monthly-averaged soil moistures at the beginning and the 12th months, while the difference is much smaller for θ at the 12th and 24th months, indicating the decay of UIC. Similarly, the soil moistures from different realizations gradually get closer to each other. As shown in Fig. 3(c), *PC* and S_p values gradually decrease with the simulation time, and their values are approximately the same after t>6 months. The significant difference at the beginning (*PC* of 4.7% and S_p of 2.6%) is due to different initial soil moistures given by the Spin-up and Monte-Carlo methods. The result indicates that the widely-used Spin-up method and Monte-Carlo method are equivalent in terms of quantifying UIC. We will use Monte-Carlo method for the rest of the study since it is consistent with the data assimilation approaches used in this study.

The determination of the threshold value when UIC is regarded to have negligible effects on modeling has been discussed in previous studies (Ajami et al., 2014; Lim et al., 2012; Seck et al., 2014). *PC* or S_p values of 1% (Yang et al., 1995), 0.1% (de Goncalves et al., 2006), or 0.01 % (Henderson-Sellers et al., 1993) have been used. As shown in Fig. 3(c), there is a significant diversity of the results between Spin-up and Monte-Carlo methods at index value of 1%, indicating that UIC still plays a significant role. In contrast, the requested t_{wu} is more than 15 months for a value of 0.1%. To balance the estimation accuracy and computational cost, we recommend a threshold of 0.5% for both Spin-up and Monte-Carlo methods, and the corresponding warm-up time t_{wu} is 8 months, which is sufficiently long for UIC to diminish and the difference between *PC* and S_p is insignificant.

3.2.2 The influencing factors on UIC

The Monte-Carlo method is used in this part to obtain the warm-up time t_{wu} and a number of scenarios are constructed under a variety of conditions (different soils, meteorological conditions, and soil profile lengths). First, the influence of soil texture and meteorological condition on t_{wu} are examined. Four different types of homogeneous soils (Sand, Loam, Silt and Clay loam listed in Table 1) and a heterogeneous soil with multiple layers (consists of Loam (0-75 cm), Clay loam (75-150 cm), Silt (150-225 cm), and Sand (225-300 cm)) under three typical meteorological conditions (M-AC, M-SC and M-HC) are employed in these scenarios, while the other model inputs use the default values (see Table 2). Besides, the influence of different soil profile lengths (1 m, 3 m, 5 m, 10 m, 15 m, and 20 m) on UIC is also investigated.

a. The influences of soil texture and meteorological condition

Fig. 4 plots t_{wu} with five different soils under three typical meteorological conditions. The computational times vary greatly according to soil property. We find that t_{wu} of Sand are all less than one day, whereas t_{wu} of Loam are 412 days, 242 days, and 195 days respectively. In addition, the warm-up times of Silt and Clay loam with M-AC and M-SC exceed 10 years, while those with M-HC are 264 days and 253 days. The results imply that the warm-up time t_{wu} for the fine-textured soil is larger than that for coarse-textured soil. This may attribute to the diversity of the drainage property for different soils. For Sand, due to its fast drainage property, the soil moisture ensemble converges extremely quickly and most of the values at the profile are maintained as residual soil moisture. Thus, the UIC of Sand disappears very fast. In contrast, the soil moisture states for Silt and Clay loam change more slowly than Sand during the simulation. Therefore, faster drainage property leads to a smaller warm-up time.

In addition, the meteorological condition has a strong impact on UIC. For example, with soil Loam, the order of t_{wu} is M-HC<M-SC<M-AC. For Silt and Clay loam, t_{wu} of M-AC and M-SC decrease from more than 10 years to 264 days and 253 days with a humid climate M-HC, respectively. With intensive and excessive rainfall events, θ approaches to the saturated soil moisture, leading to a sudden drop of S_p. Thus, the meteorological condition, especially the precipitation, plays an important role in the propagation of UIC. Moreover, regarding the heterogeneous soil with multiple layers, the t_{wu} under the M-AC is larger than 10 years (similar to Silt and Clay loam), while that under M-SC or M-HC becomes much smaller (higher than that of Loam but they are of the same magnitude). Thus, it is conjectured that t_{wu} is determined by the fine soil texture in the layered profile under dry meteorological condition, but averaged soil hydraulic properties under wet meteorological condition.

It should be noted that the t_{wu} is also relevant to the initial state of soil. Regarding the initial condition in an extremely dry state under the arid climate, the hydraulic conductivity is very small, and the initial spread extends for a long time. For instance, t_{wu} of sand increases from 1 day to 8 days when the ensemble mean value of initial soil moisture decreases from 0.2375 to 0.15 (results not shown). Yet, if a sufficiently large rain event takes place, the soil moisture increases and then converges to a similar state rapidly.

b. The influence of soil profile length

To investigate the effects of soil profile length on warm-up time, we investigate the t_{wu} values for simulations with various soil profile lengths. As presented in Fig. 5(a), the t_{wu} for soil lengths of 1 m, 3 m, 5 m, 10 m, 15 m and 20 m are 0.11 year, 0.57 year, 0.74 year, 1.57 years, 2.78 years and 4.3 years respectively, indicating that the warm-up time increases with increasing depth of soil column. Fig. 5(b) plots the t_{wu} value for each depth with the profile length of 20 m, showing that a longer warm-up time is needed if the soil layer is deeper. Both subfigures imply that UIC decays more slowly if the effects of boundary condition become less important. We also examine the case for substituting free drainage boundary for a prescribed groundwater table. The results indicate that the t_{wu} is further shortened due to the influence of bottom saturation condition (not shown).

In addition, t_{wu} in homogeneous loam reveals a power law relationship with the length of soil profile. According to the fitted curve in Fig. 5(a), the warm-up time t_{wu} is more than seven years for a depth *d* of 30 m (e.g., North China Plain, (Huo et al., 2014)) and 700 years for *d*=1000 m (e.g., Yucca Mountain Site, (Flint et al., 2001)) with loam soil. This result suggests that we should be very careful to deal with simulation with a long unsaturated profile, where the UIC lasts for an extremely long time and influence the simulation/data assimilation results.

3.3. Initialization of data assimilation

Besides IC-HfSatu, two other common methods to prescribe initial conditions in variably saturated flow model based on the availability of information are also considered in this study, including a linear interpolation between observations (at depths of 10 cm, 80 cm, 150 cm, 220 cm and 290 cm) at the beginning of simulation (IC-ObsInt) and a steady-state soil moisture profile by warming up the model with a constant infiltration flux of 1 mm/d (IC-Flux). Moreover, we employ two warm-up methods, which give initial conditions by running the model prior to the beginning of simulation period with available meteorological data (as shown in Fig. 2). If the previous meteorological data before the simulation period is available, it is used in the warm-up method (IC-WUP); otherwise, we use the meteorological data at the experimental period as a surrogate (IC-WUE). The length of warm-up time for IC-Flux, IC-WUP and IC-WUE is equal to t_{wu} (242 days) based on the results in Section 3.2.2(a), so the warming-up period of WUP for these three methods is from day 124 to day 365. In addition, IC-HfSatu and IC-ObsInt are assumed to be deterministic without uncertainty, while for the IC-Flux, IC-WUP and IC-WUE, the uncertainty of states are introduced by warming up the model with uncertain parameters.

Thus, a total of five initialization methods (IC-HfSatu, IC-ObsInt, IC-NetFlux, IC-WUP and IC-WUE) are assessed to investigate the effect of UIC on model state and parameter estimations within two data assimilation frameworks (EnKF and IES). The initial realizations of soil hydraulic parameters K_s, α and n for all data assimilation models as well as the warming-up models IC-Flux, IC-WUP and IC-WUE are generated following logarithm normal distributions, with mean values of 4.7 md^{-1}, 8.6 m^{-1} and 1.8, and variances (log-transformed) of 0.1, 0.3 and 0.006. The saturated soil moisture θ_s and residual soil moisture θ_r are assumed to be deterministic with the value of 0.43 and 0.078. Compared with the reference values (K_s, α and n for Loam are 0.2496 md^{-1}, 3.6 m^{-1} and 1.56) listed in Table 1, the prior means of unknown parameters are biased.

3.3.1 General description for various data assimilation cases

Several test cases are conducted to explore the effects of initialization on parameter estimation under various data assimilation frameworks. Case 1 investigates the effects of five initialization methods on individual parameter estimation with EnKF and IES, respectively. Then, we increase the ensemble size of IC-HfSatu and IC-ObsInt to 500 (hereafter referred to as IC-HfSatu-500 and IC-ObsInt-500) in Case 2 to demonstrate the impacts of ensemble size. Case 3 explores the effects of the uncertainty magnitude of the initial ensemble on the parameter estimations. A Gaussian noise with a standard deviation of 0.017 (counted from IC-WUP) is added to both IC-HfSatu-500 and IC-ObsInt-500 (hereafter referred to as IC-HfSatu-500-Un and IC-ObsInt-500-Un). Furthermore, to find out the role of initial condition in multi-parameter inverse problems, Case 4 is conducted to estimate K_s, α and n simultaneously. Case 5 is implemented with a simulation time of 60 days to explore the influence of assimilation time on multiple parameter estimation with IES. It should be noted that the warm-up methods (IC-WUP and IC-WUE) used in IES warm up model before every iteration (as presented in Fig. 1(b)), since the initialization of

IES by warming up the model for only the first iteration leads to poor assimilation results.

The synthetic observations used for data assimilation are generated by running the model with "true" parameter (Loam) and "true" initial condition (produced by warming up model with a sufficient long time of 10 years). The generated observations are perturbed by a Gaussian noise with a standard deviation of 0.01. A total number of 37 observations are assimilated into the model. The observation depth is at z = 10 cm and the observed soil moisture is assimilated every 10 days, starting from day 3. The details of the model inputs for Case 1 to Case 5 are listed in Table 3.

3.3.2 Result

The results for parameter estimation (lnK_s) using the two data assimilation frameworks with different initialization methods (Case 1) are compared in Fig. 6. In Fig. 6(a), the estimated lnK_s values of EnKF are presented. In general, the lnK_s estimations under different initial conditions all gradually approach the "true" values over assimilation time, but the final assimilation results are different. For IC-HfSatu, because the initial profile is uniform and arbitrarily specified, the assimilation results are affected by the parameter uncertainty and UIC simultaneously. Thus, the decreasing of $RMSE_{\mathrm{m}}$ is the slowest and the final parameter estimation result is the worst. In contrast, the initial conditions generated by warm-up methods (IC-WUP and IC-WUE) can eliminate the UIC in advance, and thus data assimilation can handle parameter uncertainty more efficiently, leading to the best results among the five. The data assimilation results of IC-WUE are a little worse than those of IC-WUP owing to the diversity of meteorological condition. Since IC-ObsInt and IC-Flux are created by adding observation information or simple infiltration information, they perform better than that with IC-HfSatu but worse than warm-up methods. Similarly, the assimilation results for IES with IC-WUP are also the best, while those with IC-HfSatu have the worst parameter estimation in the five initialization methods (Fig. 6(b)). In addition, by comparing Figs. 6(a) and 6(b), the cases using IES shows better results than those using EnKF, indicating a superior ability for IES to estimate individual parameter in variably saturated model. However, since IES estimates parameter iteratively, it has a much larger computational cost than EnKF when using warm-up methods.

For data assimilation problem, the ensemble variance is increasingly underestimated over time/iteration, which may cause the filter inbreeding problem (Hendricks Franssen and Kinzelbach, 2008).

To determine if our data assimilation runs are affected by filter inbreeding, the temporal change of the standard deviation of estimated lnK_s are plotted in Figs. 6(c) and 6(d). In general, the standard deviation of estimated lnK_s decline gradually with assimilation steps (EnKF) or iteration steps (IES). As given in Figs. 6(a) and 6(c), the filter inbreeding might take place after 280th days for EnKF, since the standard deviation of ensemble all approach to 0.1 and the estimated parameters stay constant over time. However, with the help of a damping parameter, the filter inbreeding problem for IES could be reduced significantly. This partly explains the inferior result of EnKF compared to IES.

Increasing the ensemble size and model uncertainty is an efficient approach to reduce the filter inbreeding (Hendricks Franssen and Kinzelbach, 2008). To demonstrate the impacts of ensemble size and initial uncertainty on data assimilation results, the results of lnK_s estimations utilizing the initial condition IC-HfSatu and IC-ObsInt with the ensemble size of 500 (Case 2) and a Gaussian noise (Case 3) are plotted in the Fig. 7.

The results of IC-HfSatu-500 and IC-ObsInt-500 with the ensemble size of 500 in Fig. 7 are similar with those of IC-HfSatu and IC-ObsInt (Fig. 6), indicating that the improvement of the parameter estimation result is slight when the ensemble size increases from 300 to 500. Hence, the ensemble size of 300 is sufficient for data assimilation problem in this study. In contrast, the influences of adding the uncertainty to the initial state on parameter estimation are totally different for EnKF and IES. Compared with the results of IC-ObsInt-500 and IC-HfSatu-500, the results of lnK_s estimation with IC-ObsInt-500-Un and IC-HfSatu-500-Un improve for EnKF (Fig. 7(a)), but deteriorate for IES (Fig. 7(b)). This may attribute to the diversity between two algorithms. EnKF is a sequential algorithm, so the state uncertainty introduced by UIC could decrease over assimilation steps. A larger ensemble state variance implemented at the beginning leads to a larger trust on data and thus a quicker update of parameter to truth, and can prevent EnKF from inbreeding, leading to a better result than that with initial condition of small variance. On the contrary, IES is a batch optimization method. The uncertainty of initial state exists at each iteration and has a negative effect on the model calibration during the whole simulation, worsening the parameter estimation results. Besides, we also investigate the influences of spatial correlation of the added noise (e.g., with correlation length of 50 cm or infinity) for constructing IC-HfSatu and IC-ObsInt, but their parameter estimation results are similar (not shown), indicating that the effects of spatial correlation of noise during the construction of IC-HfSatu and IC-ObsInt are not significant on parameter estimation.

Moreover, the parameter estimation results of IC-WUP are still superior to those of IC-HfSatu-500-Un and IC-ObsInt-500-Un even they all have a similar computational cost, showing the promising performance of warm-up methods. The results are reasonable since all ensemble Kalman filter methods are affected by the quality of the auto-covariance matrix and the mean value of predicted state ensemble (Eqs. (12) and (13) for EnKF; Eqs. (15) and (16) for IES). For WUP method, the initial condition is constructed by warming up the model with the prior parameter, thus IC-WUP contains useful information of prior parameter, even it is biased. Besides, the state covariance matrix is implicitly inflated due to the introduction of uncertain prior parameter ensemble during warming up. These two aspects ensure the robust performance of warm-up methods. However, the initial state ensembles of IC-HfSatu-500-Un and IC-ObsInt-500-Un are independent from the prior parameter, which introduces additional uncertainties, making the data assimilation results worse. Therefore, even using a larger ensemble size and enlarging the state uncertainty (covariance inflation), warm-up methods are still the optimal choice for both EnKF and IES algorithms. We also construct another case with a larger parameter uncertainty to alleviate filter inbreeding problem and the data assimilation for all cases are improved (not shown). The results also agree with our conclusion that WUP performs the best among the five initialization methods.

To evaluate the effects of UIC in multi-parameter inverse problem, the *RE* results of K_s, α, and n estimates of Case 4 are presented in Fig. 8. In general, the *RE* results of n and K_s are small no matter using EnKF or IES, while the *RE* of α is the largest. A cross-correlation analysis indicates that soil moisture observations are insensitive to parameter α with a free drainage boundary condition, which agrees with the results of Hu et al., (2017). In Fig. 8(a), similar to the conclusion of one-parameter inverse problem, the parameter estimation results of K_s and α with IC-HfSatu and IC-ObsInt are worse than those of IC-WUP and IC-WUE. There is not much difference between the n estimates under various initial conditions, implying that n is less affected by UIC when estimating K_s, α and n simultaneously. Compared with EnKF, IES shows a smaller *RE* (Fig. 8(b)) for all parameters, indicating IES can also perform better in multi-parameter inverse problem. However, the assimilation results with various initialization methods do not show much difference, implying that the final *RE* values are not significantly affected by UIC, possibly due to abundant observations available over one year. Nevertheless, long-term observation data may not be available in many cases.

To examine the impact of assimilation time on parameter estimation with IES, Case 5 with shorter assimilation period (60 days) and a fewer number of observations (i.e., 6) is conducted. Fig. 9 shows the *RE* results and it is inferior to those in Case 4, where the simulation time is one year (Fig. 8(b)). Nevertheless, the effects of assimilation time on parameter estimation are different for different parameters. For instance, parameter n can still be estimated well in the most of the situations. In addition, though the assimilation results of K_s degraded with a 60-day simulation, the variation of K_s estimation values among different initialization methods is small. The number of observation can greatly affect the estimation of parameter α, since *RE* of α in Case 5 (3.5, 4.8, 1.17, 0.79, and 0.23) is much larger than those in Case 4 (0.16, 0.29, 0.68, 0.24, and 0.31). Furthermore, the warm-up methods show the best data assimilation results among the five when the observations are insufficient.

4. Field validation

Synthetic observation in previous section is generated by running the model with exactly known uncertainty sources. By conducting synthetic experiments, we can thoroughly analyze the impact of UIC during data assimilation, with scenarios having different numbers of observations/unknown parameters, and more decisive conclusions can be drawn. In contrast, the field observations contain additional uncertainties which are largely unknown (e.g., the calculated evapotranspiration is inaccurate for real-world case). In order to examine the real-world applicability of the conclusions drawn from synthetic case, Field data are necessary to validate our results. A field experiment is conducted in the irrigation-drainage experimental site of Wuhan University (Li et al., 2018) (Fig. 10(a)). Meteorological data, including air temperature, relative humidity, atmospheric pressure, incident solar radiation, and precipitation, is continuously monitored by an automatic weather station (LoggerNet 4.0), which can be used as upper boundary condition after the calculation of the potential evaporation (Penman-Monteith's equation) on the bare soil (see Fig. 11(a)). A vertically-inserted frequency domain reflectometry (FDR) tube was used to monitor soil moisture (Fig. 10(b)). The in-situ soil moisture observation was measured every 3 days. The tube gave soil moisture measurements at the depths of 10, 20 and 30 cm. During 18th April 2017 to 30th May 2017, the measurements were repeated 14 times and 42 soil moisture data were collected (see Fig. 11(b)). Besides, the soil moisture at the depth of 10 cm, 20 cm, 30 cm, 40 cm, 60 cm and 80 cm at the beginning of the simulation time is also available to construct an initial profile via IC-ObsInt.

4.1 General description of the experimental case

To analyze the experimental data, the 1-D numerical domain is set as 2 m and discretized in 50 grids. The top 40 grids have a size of 2.5 cm and the rest has a size of 10 cm. The upper boundary is set as an atmospheric boundary using the data shown in Fig 11(a) and the bottom boundary is set to be free drainage since the groundwater table is much deeper than the bottom of the domain.

The prior parameter distributions follows the study of Li et al. (2018). The saturated soil moisture θ_s and residual soil moisture θ_r are given as 0.43 and 0.078, while the other hydraulic parameters are to be estimated. The initial means of K_s, α and n are set as 1 md^{-1}, 5 m^{-1} and 2, and the initial natural logarithmic variances of them are set as 0.22, 0.16 and 0.003. The data from 18th April through 27th April are used for calibration, while the remaining data are reserved for validation. The climate of Wuhan is semi-arid conditions and the soil of experimental site is sandy loam. We use a warm-up time of 242 days based on our investigation in Section 3.2.2.

4.2 Results

The assimilation results with four different initialization results (IC-HfSatu, IC-ObsInt, IC-Flux and IC-WUP) are presented in this part. Since the true hydraulic parameters at the experimental site are unknown, we assess the estimation by comparing the predicted (using estimated parameters) and observed soil moistures during the validation period. The $RMSE_{obs}$ for soil moisture predictions under different assimilation scenarios are listed in Table 4. Generally speaking, $RMSE_{obs}$ with IC-WUP are again the smallest, while IC-HfSatu has the largest $RMSE_{obs}$ values.

In order to evaluate the overall performances of the four initialization methods, the soil moisture observations and predictions at all depths are plotted in Fig. 12. The coefficients of determination under the four scenarios are 0.033, 0.599, 0.083 and 0.553, and the $RMSE_{obs}$ are 0.045, 0.037, 0.036, and 0.028 respectively. As shown in Fig. 12(a) and Fig. 12(c), IC-HfSatu and IC-Flux show very large scattering, indicating a bad prediction performance. A significant improvement is found in IC-WUP with a large R^2 and the smallest $RMSE_{obs}$ value, as shown in Fig. 12(d). Surprisingly, IC-ObsInt has the largest R^2 among the four methods, though its $RMSE_{obs}$ value is bigger than that of IC-WUP. The simulation of real-world problems may have uncertainties that are not considered in data assimilation. For instance, the meteorological data prior to the simulation for warming up is not precise from the weather-station instrument error and calculation of evapotranspiration, which has a detrimental effect on IC-WUP. IC-ObsInt, on the other hand, takes the advantage that it utilizes the soil moisture observations for both initialization and predictions. However, IC-ObsInt may not be applicable when soil moisture observations at t=0 are not available or the soil moisture profile is discontinuous in layered soils, leading to a large interpolation error. In summary, for both the synthetic and field cases, models initialized using the warm-up method result in low uncertainty and superior soil moisture predictions even if the calibration data are insufficient.

5. Discussion and Conclusions

The study investigates the effects of UIC on variably saturated flow simulations subject to different soil hydraulic parameters, meteorological conditions and soil profile lengths. Two common approaches (Spin-up and Monte-Carlo methods) are applied to explore the required warm-up time t_{wu} and temporal behavior of UIC. In addition, the data assimilation performances with five common initialization approaches are compared using synthetic experiments and a field soil moisture dataset.

Under atmospheric boundary condition, the soil moisture value near the upper boundary could approach its upper and lower bounds (saturated water content and residual water content) due to rainfall and evaporation. This significantly reduces the UIC of soil moisture profile near the soil surface. Our investigation shows that the coarse-textured soil results in faster reduction of soil moisture UIC because of fast redistribution of water in sandy soil. Regarding the influence of boundary conditions, we find that heavy rainfall can reduce UIC significantly, while an initial condition in a drier status leads to a growth of t_{wu}, since a drier soil drains and evaporates less water, making UIC of soil moisture dissipates slowly. The conclusion agrees with the conclusions reported by Castillo et al., (2003) and Seck et al., (2014). Although t_{wu} for sandy soil is very small, it could be very large for other soils (less than one day versus more than 10 years in Fig. 4). The length of soil profile plays an important role in UIC since UIC decays from the boundaries. As a result, UIC could exist persistently in a very thick vadose zone. Our findings imply that UIC dissipation depends nonlinearly on soil type, meteorological condition, and soil profile lengths, and special attention should be paid to during vadose zone modeling.

Ideally, the initial ensemble should represent the error statistics of the initial guess for the model state during data assimilation (Evensen, 2003). Thus, effort should be invested to reduce the impact of UIC on data assimilation. Methods which do not consider the UIC (i.e., assuming an initial ensemble arbitrarily without uncertainty, which was used in some studies, e.g., Shi et al., 2015) can induce significant bias according to our data assimilation results. By constructing initial condition using the information of observations or boundary condition (averaged flux), the data assimilation results can be improved. However, these two initialization methods are also suboptimal, due to the oversimplification to the complex initial condition. By warming up model with available meteorological data, the initialization methods can improve data assimilation results. Moreover, EnKF is more sensitive to filter inbreeding problem than IES. The initial condition with a larger state uncertainty gains better performance than that without covariance inflation for EnKF. While for IES, this inflated uncertainty cannot decrease over iterations, making the results inferior.

In this study, we only use the soil moisture observations rather than pressure head to construct the initial profile. For homogeneous soil column, there is a one-to-one relationship between the spread of soil moisture and pressure head (i.e., UIC in terms of pressure head can be converted from that of soil moisture). The situation will be much more complex if the soil is heterogeneous, since a large number of unknown hydraulic parameters may introduce significant nonlinearity during the transformation between head and soil moisture. For instance, the soil moisture profile is discontinuous in layered soils. The use of pressure head instead of soil moisture as initial condition for heterogeneous soils deserves investigation in our future work.

Our work leads to the following major conclusions:

1. Spin-up method and Monte-Carlo method can both quantify UIC and they agree well with each other after a sufficiently long simulation. A threshold of 0.5% for percentage cutoff *PC* or ensemble spread S_p is recommended to determine the warm-up time.

2. Warm-up time varies nonlinearly with soil textures, meteorological conditions, and soil profile length. Under most situations (e.g., Loam with the soil profile length less than 5 m under non-arid climate), one-year warm-up time is sufficient for soil water movement modeling, but an extremely long time (exceeds 10 year) is needed to warm up the model for a long, fine-textured soil profile under an arid meteorological condition.

3. IES shows better performance than EnKF in the strongly nonlinear problem and is affected less by the UIC with a long-period of observations. In addition, covariance inflation of initial condition could improve the data assimilation results for EnKF, but deteriorate them for IES.

4. The following procedure is recommended to initialize soil water modeling: 1) Evaluate the approximate warm-up time based on the model settings; 2) Initialize the model using the method of WUP (if meteorological data are available) and make sure the warming up time is larger than the required t_{wu}; 3) Run the simulation with the initial condition obtained in step 2. WUE is an alternative to WUP if the preceding meteorological data are not available. ObsInt is also a practical choice if dense soil moisture observations at the beginning of simulation are available.

Further research may examine the performance of these initialization methods in two- or three-dimensional variably saturated flow conditions. Our approach can also be extended to other modeling and data assimilation problems in other disciplines (e.g., groundwater flow and solute transport modeling, and soil-water-crop modeling).

Data/code availability. All the data used in this study can be requested by email to the corresponding author Yuanyuan Zha at zhayuan87@gmail.com.

Author contribution: Yuanyuan Zha and Jinzhong Yang developed the new package for soil water flow modeling based switching the primary variable of numerical Richards' equation; Danyang Yu and Yuanyuan Zha developed EnKF and IES codes for data assimilation of variably saturated flow, and designed and conducted the numerical cases and field data validation for this study. Seven of the co-authors made non-negligible efforts preparing the manuscript.

Competing interests: The authors declare that they have no conflict of interest.

Acknowledgments

This work is supported by Natural Science Foundation of China through grants No. 51609173 and 51779179. The authors appreciate Michael Tso (Lancaster University, U.K.) for editing the manuscript. We thank the three reviewers for their constructive comments and suggestions.

References

Ajami, H., McCabe, M. F., Evans, J. P., and Stisen, S: Assessing the impact of model warm-up on surface water-groundwater interactions using an integrated hydrologic model. Water Resour. Res., 50, 1–21, doi:10.1002/2013WR014258, 2014.

Ataie-Ashtiani, B., Volker, R. E. and Lockington, D. A.: Numerical and experimental study of seepage in unconfined aquifers with a periodic boundary condition, J. Hydrol., 222(1-4), 165–184, doi:10.1016/S0022-1694(99)00105-5, 1999.

Bauser, H. H., Jaumann, S., Berg, D., and Roth, K.: EnKF with closed-eye period - Towards a consistent aggregation of information in soil hydrology, Hydrol. Earth Syst. Sci., 20(12), 4999–5014, doi:10.5194/hess-20-4999-2016, 2016.

Carsel, R. F. and Parrish, R. S.: Developing joint probability distributions of soil water retention characteristics, Water Resour. Res., 24(5), 755–769, doi:10.1029/WR024i005p00755, 1988.

Castillo, V. M., Gómez-Plaza, A. and Martínez-Mena, M.: The role of antecedent soil water content in the runoff response of semiarid catchments: A simulation approach, J. Hydrol., 284(1-4), 114–130, doi:10.1016/S0022-1694(03)00264-6, 2003.

Chanzy, A., Mumen, M. and Richard, G.: Accuracy of top soil moisture simulation using a mechanistic model with limited soil characterization, Water Resour. Res., 44(3), 1–16, doi:10.1029/2006WR005765, 2008.

Chen, Y. and Oliver, D. S.: Levenberg-Marquardt forms of the iterative ensemble smoother for efficient history matching and uncertainty quantification, Comput. Geosci., 17(4), 689–703, doi:10.1007/s10596-013-9351-5, 2013.

Chirico, G. B., Medina, H., & Romano, N.: Kalman filters for assimilating near-surface observations into the Richards equation - Part 1: Retrieving state profiles with linear and nonlinear numerical schemes, Hydrol. Earth Syst. Sci., 18(7), 2503–2520, doi:10.5194/hess-18-2503-2014, 2014.

Cosgrove, B. A., Lohmann, D., Mitchell, K. E., Houser, P. R., Wood, E. F., Schaake, J. C., Robock, A., Sheffield, J., Duan, Q. Y., Luo, L. F., Higgins, R. W., Pinker, R. T. and Tarpley, J. D.: Land surface model spin-up behavior in the North American Land Data Assimilation System (NLDAS), J. Geophys. Res., 108, D22, doi:10.1029/2002JD003316, 2003.

Crestani, E., Camporese, M., Baú, D. and Salandin, P.: Ensemble Kalman filter versus ensemble smoother for assessing hydraulic conductivity via tracer test data assimilation, Hydrol. Earth Syst. Sci., 17(4), 1517–1531, doi:10.5194/hess-17-1517-2013, 2013.

Das, N. N. and Mohanty, B. P.: Root zone soil moisture assessment using remote sensing and vadose zone modeling, Vadose Zo. J., 5(1), 296, doi:10.2136/vzj2005.0033, 2006.

DeChant, C. M.: Quantifying the impacts of initial condition and model uncertainty on hydrological forecasts. Ph.D thesis, Portland State University, Portland, United States, 2014.

Dechant, C. M. and Moradkhani, H.: Improving the characterization of initial condition for ensemble streamflow prediction using data assimilation, Hydrol. Earth Syst. Sci., 15(11), 3399–3410, doi:10.5194/hess-15-3399-2011, 2011.

De Goncalves, L. G. G., Shuttleworth, W. J., Burke, E. J., Houser, P., Toll, D. L., Rodell, M., and Arsenault, K.: Toward a South America Land Data Assimilation System: Aspects of land surface model warm-up using the Simplified Simple Biosphere, J. Geophys. Res. Atmos., 111(17), 1–13, doi:10.1029/2005JD006297, 2006.

De Lannoy, G. J., Reichle, R. H., Houser, P. R., Pauwels, V., and Verhoest, N. E.: Correcting for forecast bias in soil moisture assimilation with the ensemble Kalman filter. Water Resour. Res., 43(9). doi:10.1029/2006WR005449, 2007.

Doussan, C., Jouniaux, L. and Thony, J. L.: Variations of self-potential and unsatureated water flow with time in sandy loam and clay loam soils, J. Hydrol., 267, 173–185, doi:10.1016/S00221694(02)00148-8, 2002

Emerick, A. A. and Reynolds, A. C.: Ensemble smoother with multiple data assimilation, Comput. Geosci., 55, 3–15, doi:10.1016/j.cageo.2012.03.011, 2013.

Erdal, D., Neuweiler, I. and Wollschläger, U.: Using a bias aware EnKF to account for unresolved structure in an unsaturated zone model, Water Resour. Res., 50(1), 132–147, doi:10.1002/2012WR013443, 2014.

Evensen, G.: The Ensemble Kalman Filter: Theoretical formulation and practical implementation, Ocean Dyn., 53(4), 343–367, doi:10.1007/s10236-003-0036-9, 2003.

Evensen, G.: Sequential data assimilation with a nonlinear quasi-geostrophic model using Monte Carlo methods to forecast error statistics, J. Geophys. Res. Oceans., 99(C5), 10143-10162. doi:10.1029/94JC00572, 1994.

Flint, A L., Flint, L. E., Bodvarsson, G. S., Kwicklis, E. M. and Fabryka-Martin, J.: Development of the conceptual model of unsaturated zone hydrology at Yucca Mountain, Nevada, Concept. Model. Flow Transp. Fract. Vadose Zo., 47–85, doi:10.1016/S0022-1694(01)00358-4, 2001.

Forsyth, P. A., Wu, Y. S. and Pruess, K.: Robust numerical methods for saturated-unsaturated flow with dry initial conditions in heterogeneous media, Adv. Water Resour., 18(1), 25–38, doi:10.1016/0309-1708(95)00020-J, 1995.

Freeze, R. A.: The Mechanism of Natural Ground-Water Recharge and Discharge: 1. One-dimensional, Vertical, Unsteady, Unsaturated Flow above a Recharging or Discharging Ground-Water Flow System, Water Resour. Res., 5(1), 153 – 171, doi:10.1029/WR005i001p00153, 1969.

French, H. K., Van Der Zee, S. E. A. T. M. and Leijnse, A.: Differences in gravity-dominated unsaturated flow during autumn rains and snowmelt, Hydrol. Process., 13(17), 2783–2800, doi:10.1002/(SICI)1099-1085(19991215)13:17<2783::AID-HYP899>3.0.CO;2-9, 1999.

Galantowicz, J. F., Entekhabi, D., and Njoku, E. G.: Tests of sequential data assimilation for retrieving profile soil moisture and temperature from observed L-band radiobrightness, IEEE. T. Geosci. Remote., 37(4), 1860-1870, doi:10.1109/36.774699, 1999.

Henderson-Sellers, A., Yang, Z.-L., Dickinson, R. E., Henderson-Sellers, A., Yang, Z.-L. and Dickinson, R. E.: The project for intercomparison of land-surface parameterization schemes, Bull. Am. Meteorol. Soc., 74(7), 1335–1349, doi:10.1175/15200477(1993)074<1335:TPFIOL>2.0.CO;2,1993.

Hu, S., Shi, L., Zha, Y., Williams, M. and Lin, L.: Simultaneous state-parameter estimation supports the evaluation of data assimilation performance and measurement design for soil-water-atmosphere-plant system, J. Hydrol., 555, 812–831, doi:10.1016/j.jhydrol.2017.10.061, 2017.

Hendricks Franssen, H. J. and Kinzelbach, W.: Real-time groundwater flow modeling with the Ensemble Kalman Filter: Joint estimation of states and parameters and the filter inbreeding problem, Water Resour. Res., 44(9), 1–21, doi:10.1029/2007WR006505, 2008.

Huang, C., Li, X., Lu, L. and Gu, J.: Experiments of one-dimensional soil moisture assimilation system based on ensemble Kalman filter, Remote Sens. Environ., 112(3), 888–900, doi:10.1016/j.rse.2007.06.026, 2008.

Huo, S., Jin, M., Liang, X. and Lin, D.: Changes of vertical groundwater recharge with increase in thickness of vadose zone simulated by one-dimensional variably saturated flow model, J. Earth Sci., 25(6), 1043–1050, doi:10.1007/s12583-014-0486-7, 2014.

Ji, S. and Unger, P. W.: Soil water accumulation under different precipitation, potential evaporation, and straw mulch conditions, Soil Sci. Soc. Am. J., 65(2), 442, doi:10.2136/sssaj2001.652442x, 2001.

Li, B., Toll, D., Zhan, X. and Cosgrove, B.: Improving estimated soil moisture fields through assimilation of AMSR-E soil moisture retrievals with an ensemble Kalman filter and a mass conservation constraint, Hydrol. Earth Syst. Sci., 16(1), 105–119, doi:10.5194/hess-16-105-2012, 2012.

Li, C. and Ren, L.: Estimation of unsaturated soil hydraulic parameters using the Ensemble Kalman Filter, Vadose Zo. J., 10(4), 1205, doi:10.2136/vzj2010.0159, 2011.

Li, X., Shi, L., Zha, Y., Wang, Y. and Hu, S.: Data assimilation of soil water flow by considering multiple uncertainty sources and spatial–temporal features: a field-scale real case study, Stoch. Environ. Res. Risk Assess., 32(9), 2477–2493, doi:10.1007/s00477-018-1541-1, 2018.

Lim, Y.-J., Hong, J. and Lee, T.-Y.: Spin-up behavior of soil moisture content over East Asia in a land surface model, Meteorol. Atmos. Phys., 118(3-4), 151–161, doi:10.1007/s00703-012-0212-x, 2012.

Margulis, S. A., Mclaughlin, D. B., Entekhabi, D. and Dunne, S.: Land data assimilation and estimation of soil moisture using measurements from the Southern Great Plains 1997 Field Experiment, Water Resour. Res., 38(12), 1–18, doi:10.1029/2001WR001114, 2002.

Medina, H., Romano, N. and Chirico, G. B.: Kalman filters for assimilating near-surface observations into the Richards equation – Part 2: A dual filter approach for simultaneous retrieval of states and parameters, Hydrol. Earth Syst. Sci., 18(7), 2521–2541, doi:10.5194/hess-18-2521-2014, 2014a.

Medina, H., Romano, N. and Chirico, G. B.: Kalman filters for assimilating near-surface observations into the Richards equation - Part 3: Retrieving states and parameters from laboratory evaporation experiments, Hydrol. Earth Syst. Sci., 18(7), 2543–2557, doi:10.5194/hess-18-2543-2014, 2014b.

Mohamed Mumen: Caractérisation du fonctionnement hydrique des sols à l’aide d’un modèle mécaniste de transferts d’eau et de chaleur mis en oeuvre en fonctions des informations disponibles sur le sol, Ph.D. thesis, University of Avignon, Avignon, France, 2006.

Montzka, C., Moradkhani, H., Weihermüller, L., Franssen, H. J. H., Canty, M. and Vereecken, H.: Hydraulic parameter estimation by remotely-sensed top soil moisture observations with the particle filter, J. Hydrol., 399(3-4), 410–421, doi:10.1016/j.jhydrol.2011.01.020, 2011.

Mualem, Y.: Wetting front pressure head in the infiltration model of Green and Ampt, Water Resour. Res., 12(3), 564–566, doi:10.1029/WR012i003p00564, 1976.

Oliver, D. S. and Chen, Y.: Improved initial sampling for the ensemble Kalman filter, Comput. Geosci., 13(1), 13–27, doi:10.1007/s10596-008-9101-2, 2009.

Pujol, J.: The solution of nonlinear inverse problems and the Levenberg-Marquardt method, Geophysics, 72(4), doi:10.1190/1.2732552, 2007.

Rahman, M. M. and Lu, M.: Model spin-up behavior for wet and dry basins: A case study using the Xinanjiang model, Water, 7(8), 4256–4273, doi:10.3390/w7084256, 2015.

Reichle, R. H. and Koster, R. D.: Assessing the Impact of Horizontal Error Correlations in Background Fields on Soil Moisture Estimation, J. Hydrometeorol., 4(6), 1229–1242, doi:10.1175/1525-7541(2003)004<1229:ATIOHE>2.0.CO;2, 2003.

Rodell, M., Houser, P. R., Berg, A. A. and Famiglietti, J. S.: Evaluation of 10 Methods for Initializing a Land Surface Model, J. Hydrometeorol., 6(2), 146–155, doi:10.1175/JHM414.1, 2005.

Ross, P. J.: Modeling soil water and solute transport–fast, simplified numerical solutions, Agron. J., 95, 1352-1361, https://doi.org/10.2134/agronj2003.1352, 2003.

Ross, P. J.: Fast solution of Richards ’ Equation for flexible soil hydraulic property descriptions. Land and Water Technical Report, CSIRO, 39(06), 2006.

Seck, A., Welty, C. and Maxwell, R. M.: Spin-up behavior and effects of initial conditions for an integrated hydrologic model, Water Resour. Res., 51, 2188–2210, doi:10.1002/2014WR016371, 2014.

Shi, L., Song, X., Tong, J., Zhu, Y. and Zhang, Q.: Impacts of different types of measurements on estimating unsaturated flow parameters, J. Hydrol., 524, 549–561, doi:10.1016/j.jhydrol.2015.01.078, 2015.

Šimůnek, J., Šejna, M., Saito, H., Sakai, M., and van Genuchten, M. T.: The Hydrus-1D software package for simulating the movement of water, heat, and multiple solutes in variably saturated media, version

4.16, HYDRUS software series 3 Department of Environmental Sciences, University of California Riverside, Riverside, California, USA, 308 pp., 2013.

Szomolay, B.: Analysis of a moving boundary value problem arising in biofilm modelling, Math. Method Appl. Sci., 31(15), 1835–1859, doi:10.1002/mma.1000, 2008.

Tran, A. P., Vanclooster, M. and Lambot, S.: Improving soil moisture profile reconstruction from ground-penetrating radar data: A maximum likelihood ensemble filter approach, Hydrol. Earth Syst. Sci., 17(7), 2543–2556, doi:10.5194/hess-17-2543-2013, 2013.

van Genuchten, M. T., and Parker, J. C.: Boundary conditions for displacement experiments through short laboratory soil columns, Soil Sci. Soc. Am. J., 48(4), 703–708, doi:10.2136/sssaj1984.03615995004800040002x, 1984.

Varado, N., Braud, I., Ross, P. J., & Haverkamp, R.: Assessment of an efficient numerical solution of the 1D Richards' equation on bare soil, J. Hydrol., 323(1-4), 244–257, https://doi.org/10.1016/j.jhydrol.2005.07.052, 2006.

Vereecken, H., Huisman, J. A., Bogena, H., Vanderborght, J., Vrugt, J. A., & Hopmans, J. W.: On the value of soil moisture measurements in vadose zone hydrology: A review, Water Resour. Res., 46(4), 1–21. https://doi.org/10.1029/2008WR006829, 2010.

Walker, J. P. and Houser, P. R.: A methodology for initializing soil moisture in a global climate model: Assimilation of near-surface soil moisture observations, J. Geophys. Res. Atmos., 106(D11), 11761–11774, doi:10.1029/2001JD900149, 2001.

Wu, C. C. and Margulis, S. A.: Feasibility of real-time soil state and flux characterization for wastewater reuse using an embedded sensor network data assimilation approach, J. Hydrol., 399(3-4), 313–325, doi:10.1016/j.jhydrol.2011.01.011, 2011.

Wu, C. C. and Margulis, S. A.: Real-time soil moisture and salinity profile estimation using assimilation of embedded sensor datastreams, Vadose Zo. J., 12(1), doi:10.2136/vzj2011.0176, 2013.

Xie, T., Liu, X. and Sun, T.: The effects of groundwater table and flood irrigation strategies on soil water and salt dynamics and reed water use in the Yellow River Delta, China, Ecol. Modell., 222(2), 241–252, doi:10.1016/j.ecolmodel.2010.01.012, 2011.

Yang, Z. L., Dickinson, R. E., Henderson-Sellers, A. and Pitman, A. J.: Preliminary study of spin-up processes in land surface models with the first stage data of Project for Intercomparison of Land Surface Parameterization Schemes Phase 1(a), J. Geophys. Res., 100(D8), 16553, doi:10.1029/95JD01076, 1995.

Zha, Y., Shi, L., Ye, M. and Yang, J.: A generalized Ross method for two- and three-dimensional variably saturated flow, Adv. Water Resour., 54, 67–77, doi:10.1016/j.advwatres.2013.01.002, 2013.

Table 1. Soil hydraulic parameters used in simulation.

Soil	θ_s	θ_r	K_s/md^{-1}	α/m^{-1}	n
Sand	0.43	0.045	7.128	14.5	2.68
Loam	0.43	0.078	0.2496	3.6	1.56
Silt	0.46	0.034	0.06	1.6	1.37
Clay loam	0.41	0.095	0.062	1.9	1.31

Table 2. The default model settings used in the simulations.

Parameter definition	**Value or type**
Initial condition	a uniform 50% relative saturation over the soil profile (IC-HfSatu)
Number of soil layers	1
Thickness of soil zone	3 m
Soil hydraulic properties	Loam
Upper boundary	M-SC
Bottom boundary	Free drainage
Number of grids	60 (with the size of 5 cm)
Simulation time	365 days

Table 3. Case summary for parameter estimation within EnKF and IES.

Case	Description	Ensemble Size	Initial Uncertainty	Simulation Time	Framework
Case 1	Individual parameter estimation	-	-	-	EnKF/IES
Case 2		500	-	-	EnKF/IES
Case 3		500	0.017	-	EnKF/IES
Case 4	Multiple parameter estimation	-	-	-	EnKF/IES
Case 5		-	-	60	IES

Note: Ungiven values use the default values. The default value of initial uncertainty for IC-ObsInt and IC-HfSatu is 0.

Table 4. $RMSE_{obs}$ results for the soil moisture predictions at observation points with different initial conditions in the experimental case.

Initial condition	**10cm**	**20cm**	**30cm**
IC-HfSatu	0.0232	0.0271	0.0280
IC-ObsInt	0.0286	0.0187	0.0134
IC-Flux	0.0198	0.0222	0.0206
IC-WUP	0.0180	0.0153	0.0155

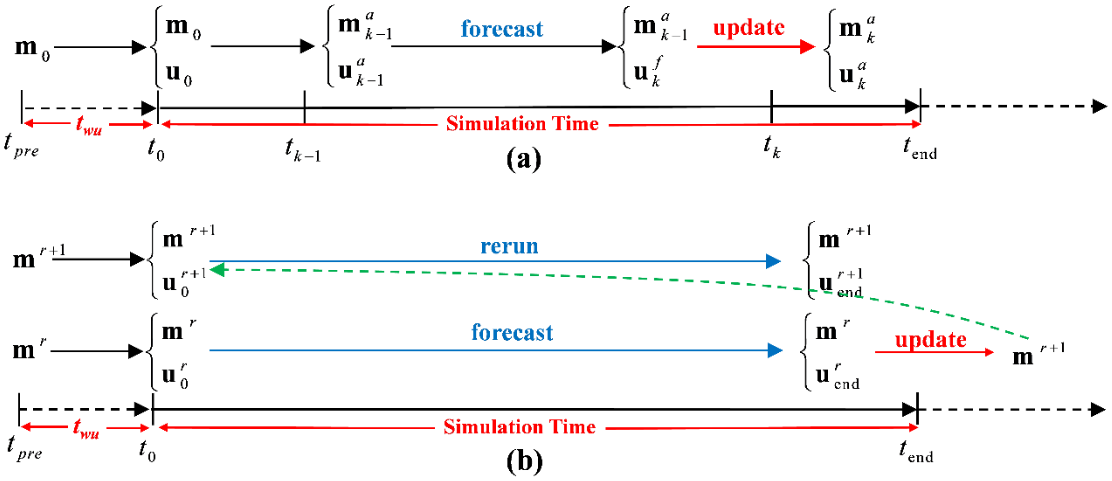

Fig. 1. Flowcharts of simulation period (or data assimilation period with (a) ensemble Kalman filter (EnKF) and (b) iterative ensemble smoother (IES)) and warming up period. t_0 is the initial time and t_{end} is the end of simulation time. $\mathbf{m}_k$ and $\mathbf{u}_k$ are the vectors of model parameters (e.g., hydraulic conductivity) and state variables (e.g., soil moisture), respectively, at time t_k, while $\mathbf{m}^r$ and $\mathbf{u}^r$ are the vectors at iteration r; the superscripts a and f refer to model analysis and forecast (or initial guess). Besides, the period between t_{pre} and t_0 donates the process of warming up, and t_{wu} is the required warm-up time.

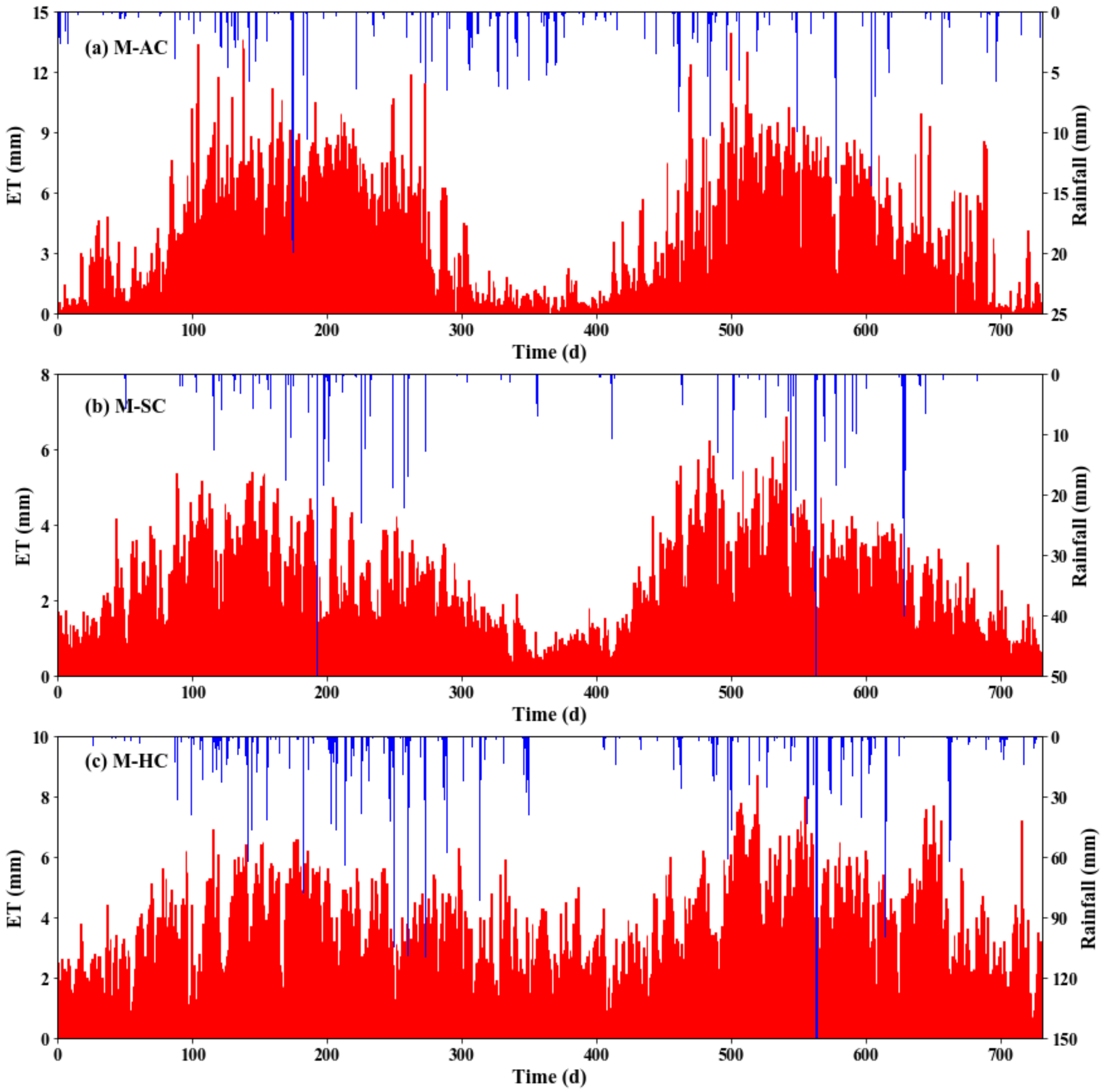

E

Fig. 2. Synthetic rainfall (blue bars) and potential evaporation (red bars) of three typical climates: (a) arid climate, (b) semi-arid climate, and (c) humid climate. It should be noted that the meteorological data of simulation period is from day 366 to day 730.

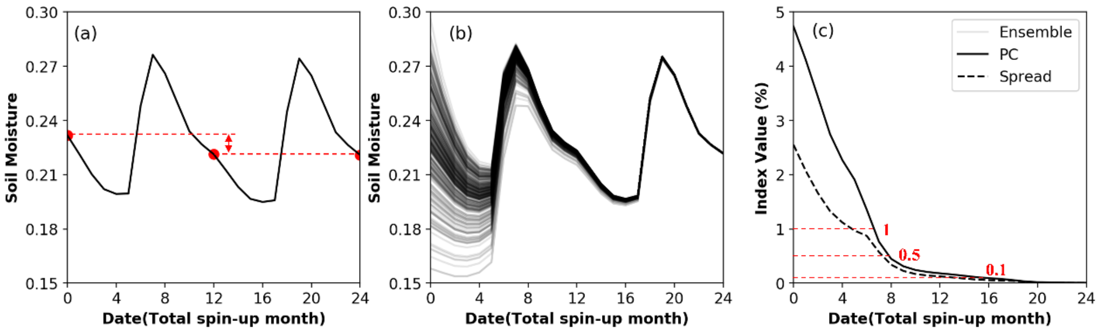

Fig. 3. Comparison of Spin-up and Monte-Carlo methods in determining warm-up time. (a) Spin-up method with monthly-averaged soil moisture versus time by running a simulation recursively for 10 years, (b) Monte-Carlo method with monthly-averaged soil moisture of different realizations versus time based on various initial conditions, and (c) Comparison of *PC* and S_p versus time. For the purpose of demonstration, the parameter uncertainty is not considered and we only show the results of the first two years in the figure.

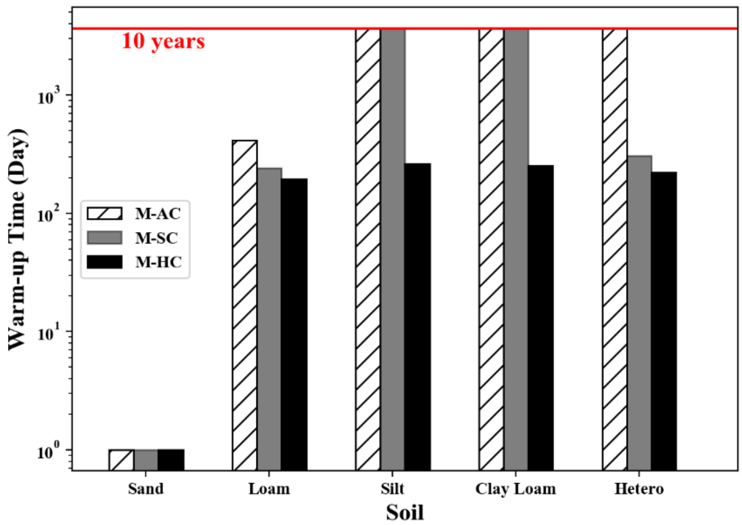

Fig. 4. The length of warm-up time t_{wu} with various soils and meteorological conditions. Note that some of the t_{wu} values are larger than 10 years and are not able to be obtained due to the 10-year simulation time. The heterogeneous soil profile consists of Loam (0-75 cm), Clay loam (75-150 cm), Silt (150-225 cm), and Sand (225-300 cm).

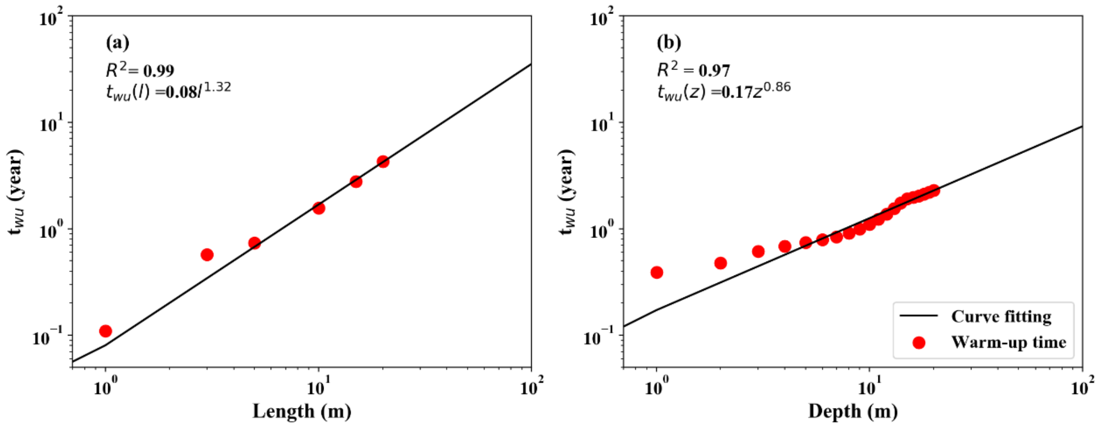

Fig. 5. The value of the warm-up time t_{wu}. (a) The overall profile t_{wu} values versus different soil profile lengths (l) and (b) t_{wu} value as a function of depth z with a 20-m soil profile.

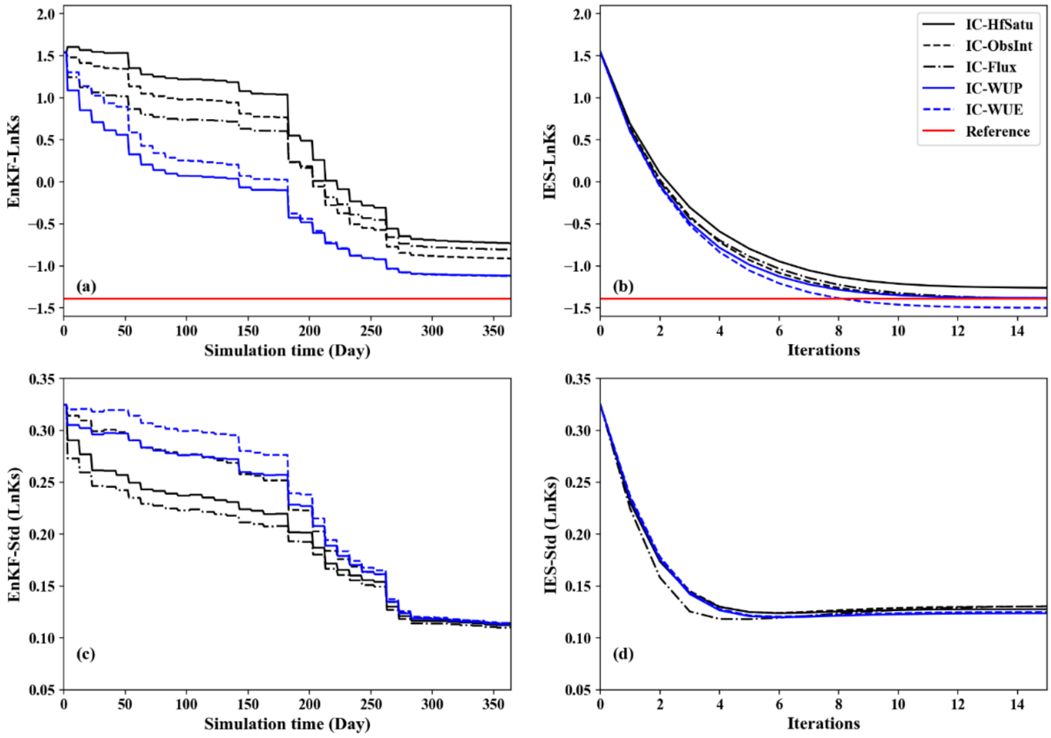

Fig. 6. The results of lnK_s estimations (first row) and their associated standard deviations (second row) within two data assimilation frameworks (left: EnKF; right: IES) under five initialization methods (Case 1).

810

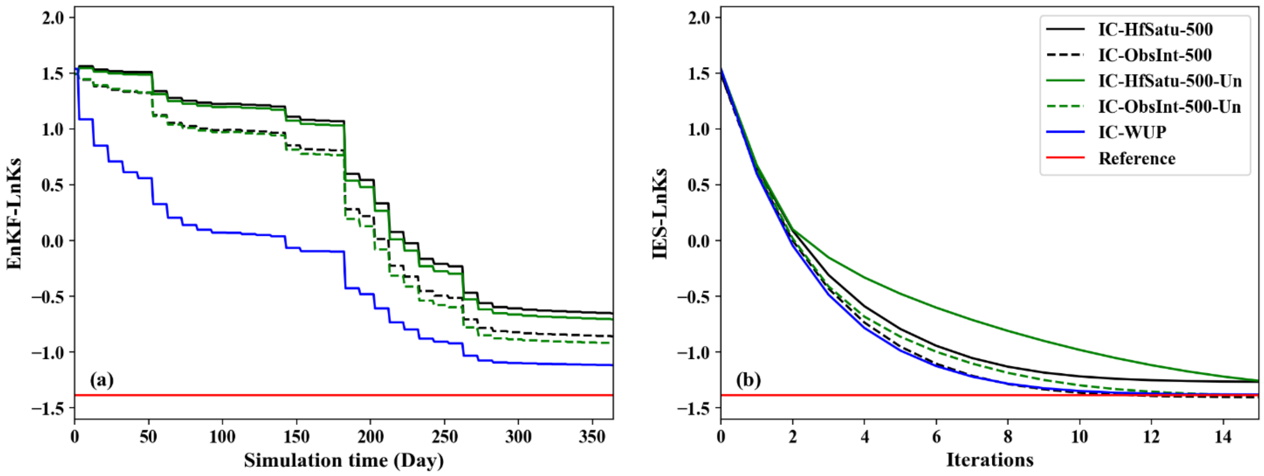

Fig. 7. The impacts of increased ensemble size (Case 2) and uncertainty of initial state (Case 3) on the results of lnK_s estimations within EnKF and IES.

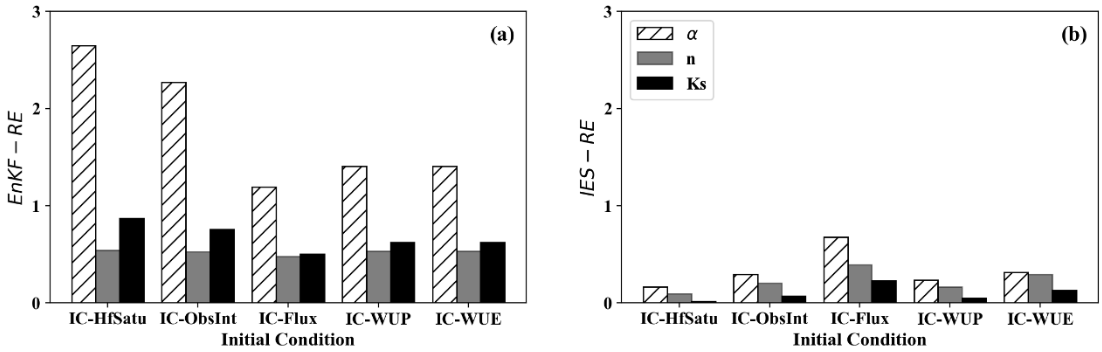

Fig. 8. The *RE* results of parameter estimations (α, n and K_s) under five initialization methods with (a) EnKF and (b) IES (Case 4).

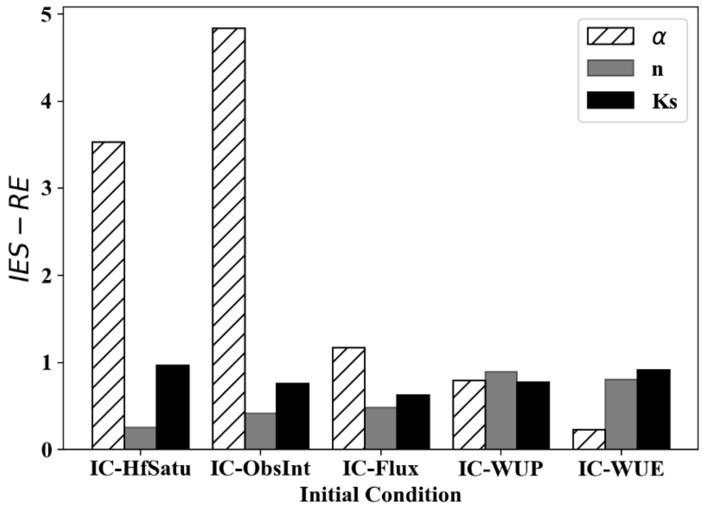

820 **Fig. 9.** The *RE* results of parameter estimations under five initialization methods with IES when the simulation time is 60 days (Case 5).

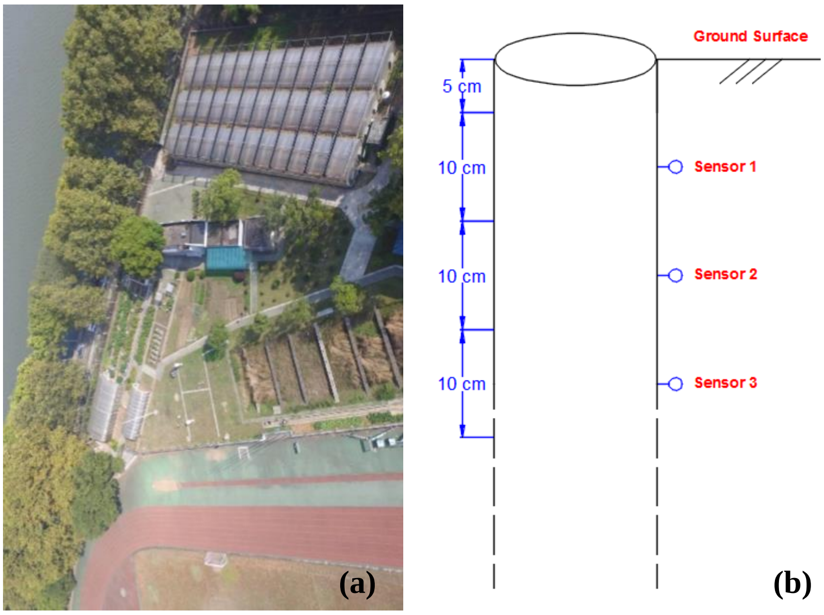

Fig. 10. The experimental site: (a) plan view, and (b) the cross-sectional view of the FDR sensor.

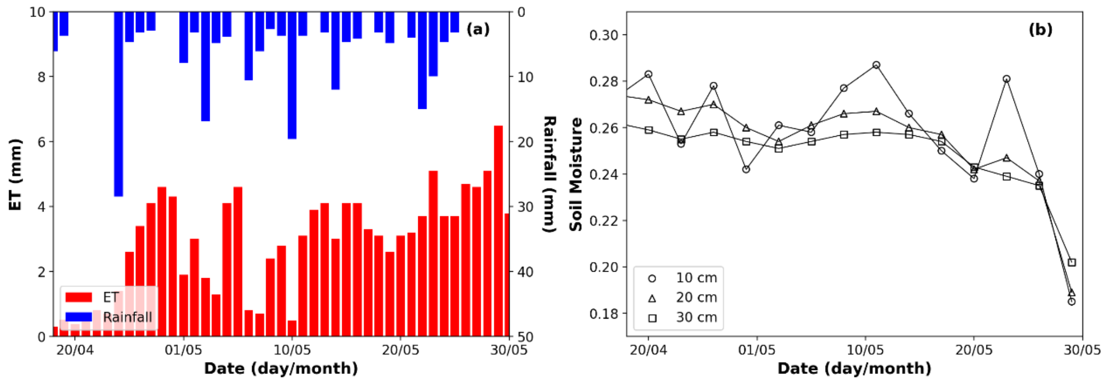

Fig. 11. The meteorological information and observed soil moistures over the experimental time. (a) Observed rainfall and calculated potential evaporation. (b) Temporal change of soil moisture data at three different observed depths (10 cm, 20 cm and 30 cm).

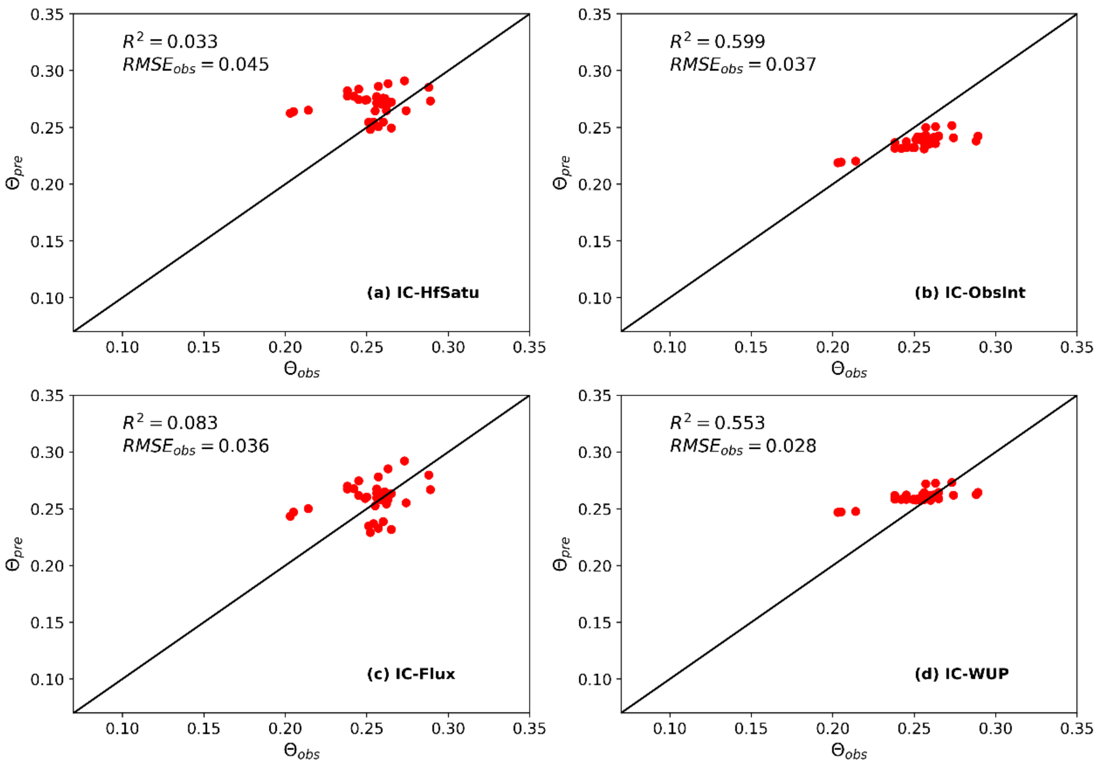

Fig. 12. The comparisons between soil moisture observations and predictions (with estimated parameters from IES combined with different initialization methods) at all observation depths.